Haddrell, A. E., Davies, J. F., & Reid, J. P. (2015). Dynamics of particle size on inhalation of environmental aerosol and impact on deposition fraction. Environmental Science & Technology, 49(24), 14512-14521. DOI: 10.1021/acs.est.5b01930

Dynamics of particle size on inhalation of environmental aerosol and impact on deposition fraction

Allen E. Haddrell*, James F. Davies, and Jonathan P. Reid

School of Chemistry
University of Bristol
Bristol, UK, BS8 1TS
Tel: 0117-331-7388
a.haddrell@bristol.ac.uk

Abstract

Inhalation of elevated levels of particulate air pollution has been shown to elicit the onset of adverse health effects in humans, where the magnitude of the response is a product of where in the lung the particulate dose is delivered. At any point in time during inhalation the depositional flux of the aerosol is a function of the radius of the droplet, thus a detailed understanding of the rate and magnitude of the mass flux of water to the droplet during inhalation is crucial. In this study, we assess the impact of aerosol hygroscopicity on deposited dose through the inclusion of a detailed treatment of the mass flux of water to account for the dynamics of particle size in a modified version of the standard International Commission on Radiological Protection (ICRP) whole lung deposition model. The ability to account for the role of the relative humidity (RH) of the aerosol prior to, and during, inhalation on the deposition pattern is explored, and found to have a significant effect on the deposition pattern. The model is verified by comparison to previously published measurements, and used to demonstrate that ambient RH affects where in the lung indoor particulate air pollution is delivered.

TOC Art

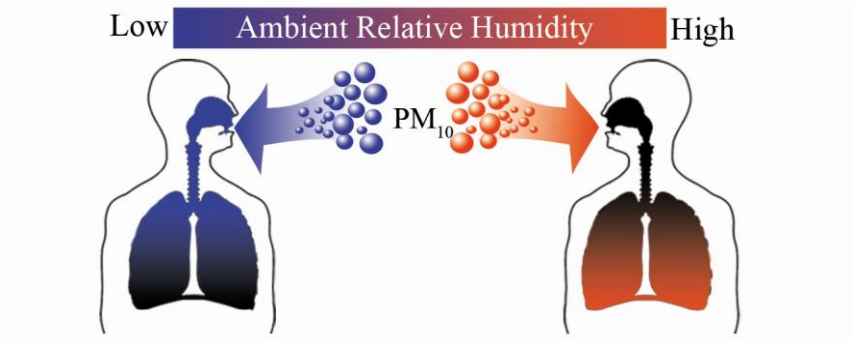

1.0 Introduction

The association between the inhalation of elevated levels of particulate air pollution and the onset of local and/or systemic adverse health effects in humans has been well established.[1, 2] The severity of the effect is correlated with the size distribution and chemical composition of the aerosol,[3] and overall exposure.[4] Several inhalation models have been used to predict dose,[5, 6] typically reporting the deposited fraction of the total aerosol population within a specific region in the lung as a function of initial aerosol diameter. There are numerous challenges in the development of these models that are both biological,[7] such as accounting for variations in lung morphology and breathing patterns, and physical, such as deposition mechanisms coupled with the fluid dynamics of aerosol transport.[8] An important factor which remains under-evaluated is the role of the chemical composition of the aerosol

particles in influencing the deposition pattern through influencing hygroscopic growth, and the influence of the environmental conditions to which the aerosol is exposed prior to inhalation.[9, 10]

The size of aerosol particles in their surrounding environment is dynamic[11] and reliant on the relative humidity (RH) in the gas-phase of the aerosol (figure 1A).[12] The absolute magnitude of the size change (the capacity for hygroscopic growth) a single droplet can experience as it drifts from one RH to another is dependent on the chemical composition of the droplet and the two RHs the droplet is transitioning between.[13] The amount of time taken for the aerosol droplet to reach equilibrium with its surrounding environment, or the rate of change of size, is governed by the kinetics of mass and heat flux to and from the droplet surface (figure 1B).[14] Thus, a detailed understanding of the thermodynamic properties and kinetic processes which control the rate and magnitude of mass transport is required to accurately model aerosol dynamics over the inhalation cycle

An aerosol particle will experience an abrupt change in RH during inhalation when the surrounding gas-phase water concentration rapidly increases due to the high humidity in the body. This sudden change in RH will in turn lead to a rapid increase in the diameter of the particle.[15] The RH experienced by the aerosol particle in the environment external to the body, termed the ambient RH, affects the size and composition of the aerosol at the point of inhalation, influencing the capacity of the aerosol to take up further water during inhalation (for example, NaCl in figure 1A). For instance, particles of identical dried solute chemical composition suspended in an atmosphere with an RH of 50% (figures 1A and 1C) have greater capacity to absorb water, changing in size by a larger proportion, than those of an identical initial diameter suspended in an atmosphere with a higher RH (figure 1D). Note that the timescale of this size change is dependent on the initial droplet diameter.

Lung models fall into one of two broad categories, either whole lung or local scale.[6] Of these, some are unable to incorporate the hygroscopic condensation that occurs during inhalation[16] while others can,[17] clearly illustrating an absence of consensus in the literature of how the hygroscopic behaviour of inhaled aerosol should be treated. Although local scale models (typically based on simulations using computational fluid dynamics (CFD)) produce more accurate predictions of aerosol deposition within the respiratory tract, validation of these models, *in vivo*, has been impossible until recently.[18, 19] Instead, local scale deposition has been confirmed using *in vitro* data.[20-22] In these studies, a portion of the upper respiratory tract is constructed (a plastic nose, mouth and/or throat),[23] aerosol introduced, and then the deposition pattern,[24] or total deposition[23] measured. Although highly useful, these *in vitro* models are limited to the upper airway and cannot probe in detail the deposition fraction in the deep lung.

Though less well defined than CFD models, whole lung models predict regional dose and can be assessed experimentally.[25, 26] The International Commission on Radiological Protection (ICRP) lung deposition model is considered the standard whole lung model for routine dosimetry assessments.[27, 28]

A model based on the traditional ICRP model is presented here to demonstrate the importance of an accurate parameterization of the hygroscopic properties of the aerosol in predicting the total and regional deposition within the lung and the importance of considering atmospheric conditions when determining aerosol dosage, and to improve the utility of the traditional ICRP model through an accurate parameterization of the hygroscopic growth kinetics during inhalation. Systems in this study range from simple salts to purely organic aerosol. The sensitivity of the regional and total dose to the RH within the lung is also considered. .

2.0 Methods

2.1 Model structure

The structure of the inhalation model developed here is that of the ICRP model (figure 2A) described in detail previously[5]; sensitivity analysis of the traditional ICRP model has been reported previously.[29-31] Only a brief description of the model will be given, followed by the specific details of the modifications developed here. The respiratory tract is divided into five separate regions: nose (extrathoracic, ET-1), mouth and throat (ET-2), bronchial (BB), bronchiolar (bb) and the alveolar-interstitial (AI) (figure 2A). During a single breath through the nose, the inhalable aerosol passes through ET-1, ET-2, BB and bb twice, once during inhalation and once during exhalation, and the AI only once. The time taken for each breath and the subsequent time taken for the aerosol to reach each region during both inhalation and exhalation are calculated based on many factors, including sex, relative body size and level of activity. The physical mechanism of particle deposition onto the lung surface occurs via diffusion and sedimentation (collectively termed thermodynamic deposition), or impaction (termed aerodynamic deposition). In each region of the lung, the fraction of all aerosol removed from the air, η, is calculated from:

Eq. 1 $$\eta = 1 - e^{-ar^p}$$

a and p are constants, and r is a function of the aerodynamic diameter of the aerosol and the air flow rate. The values of a, p and r are unique to each anatomical region and for the mechanism of deposition.[32] A table summarizing the previously reported values of a, p and r is given in Supporting Information (Table S1). Both thermodynamic and aerodynamic depositions are highly dependent on

the size of the particle. For example, in the AI region of a resting Caucasian male, the aerodynamic deposition (η_{ae}) is:

Eq. 2 $$\eta_{ae} = 1 - e^{(-0.146(2.3d_{ae}^2)^{0.6495})}$$

The thermodynamic deposition (η_{th}) is:

Eq. 3 $$\eta_{th} = 1 - e^{(-67(2.3D)^{0.6101})}$$

d_{ae} is the aerodynamic diameter of the particles and D is the diffusion coefficient of the aerosol (which itself is a function of the particle diameter). Thus it is critical to have a detailed understanding of the aerosol dynamics during inhalation to accurately predict deposition frequency. In the standard ICRP model, the parameterization of hygroscopic growth of the aerosol during inhalation is based on fits to experimental data[33] and is represented by equation 4:

Eq. 4 : $$d_{ae}(t) = (d_{ae}(\infty) \times d_{ae}(0)) - (d_{ae}(\infty) \times d_{ae}(0) - d_{ae}(0)) \times \left(\exp\left(\frac{-(10 \times t)^{0.55}}{d_{ae}(0)} \right) \right)^{0.6}$$

The meaning of these variables is given in Table 1. A value is selected for $d_{ae}(\infty)$, typically assumed to be 3.0 for hygroscopic NaCl droplets.[34] Predictions of the time dependent growth of aerosol during inhalation, using this parameterization for varying values of $d_{ae}(\infty)$ at the specific time points (where each time point is when the aerosol is in each region in the lung identified in figure 2A), are shown in figure 2B. Parameters such as the ambient RH prior to inhalation were either not considered or assumed to be inconsequential (Eq. 4).[33]

2.2 Semi-analytical treatment for hygroscopic growth kinetics of a single particle

In recent work[35-38] we have performed detailed measurements of the evaporation of water from numerous aerosol types to verify the semi-analytical solution to the mass and heat flux equations of Kulmala *et al*.[39] These continuum regime equations account for the Kelvin effect and incorporate the transition corrections factors of Fuchs-Sutugin to broaden their predictive potential into the submicron regime. The instantaneous mass flux to or from a droplet, I (units g/s), can be calculated from equation 5:

Eq. 5 $$I = -4\pi a \frac{S_\infty - a_w}{\frac{RT_\infty}{M\beta_m A D_w p_{v,\infty}} + \frac{S_a L^2 M}{R\beta_T K T_\infty^2}} \left(\frac{Sh}{2} \right)$$

The definition of these variables is given in Table 1. The method by which this equation is used to simulate the time-dependence in droplet size has been described in detail in previous publications.[35] Physically, Eq. 5 describes the continuum diffusional transport of water between the gas phase at infinite distance and the droplet surface, and the ensuing condensational (or evaporative) kinetics. Primarily this mass flux is governed by difference between the water activity within the droplet (and, thus, the droplet vapour pressure and partial pressure of water at the droplet surface) and the degree of saturation (the partial pressure of water in the gas phase) at infinite distance. In extreme cases, transport across the droplet surface may be slowed by other kinetic factors such as the presence of a surfactant coating (factored in through the transitional correction factor β_M) or through the slow diffusion of water within the bulk of the particle (not considered by equation 5).[40] Additionally, Eq. 5 accounts for the correction to the mass flux required to correct for the slow heat flux to/from the particle and the accompanying displacement in droplet temperature away from that of the gas phase.

We use equation 5 to predict the time-dependent growth kinetics of aerosol of varying composition/hygroscopic response during inhalation. The diameter of the aerosol droplets at appropriate points in time (indicative of the time reached in each region in the lung, figure 2A) were extracted and used to refine the predictions from the conventional ICRP framework. Then, the subsequent deposition fraction was estimated. Unless otherwise stated, the assumption is made that the thermal accommodation coefficient is unity; a range of values of the mass accommodation coefficient are considered (1.0 to 5.0×10^{-5}).[41] Further, it is assumed that there is no bulk limitation to mass transfer, i.e. diffusional mixing within the droplet is much more rapid than the timescale of water transport such that the particles remained homogeneous.[14] The water activity in the droplet at a particular radial growth factor is critical in determining the flux; the association between water activity and radial growth factor determines the extent (figure 1A) and rate (figure 1B) at which a given aerosol will grow following inhalation. For the inorganic aerosols studied here, the radial growth factor at a corresponding water activity is determined using the Aerosol Diameter Dependent Model (ADDEM) (Supplemental Figure 1A).[42, 43] For the organic aerosol, GF is derived using κ-Kohler theory (Supplemental Figure 1B), according to:

Eq. 6 $$GF = \sqrt[3]{1 + \frac{\kappa\, a_w}{1 - a_w}}$$

where κ is the dimensionless hygroscopicity parameter.[44] For multiple component aerosols, whether multiple inorganic or organic species (or a mixture of the two), the hygroscopic behaviour of the aerosol can be readily estimated via the Zdanovskii-Stokes-Robinson (ZSR) approach.[45-47]

A comparison of the predicted growth kinetics of pure NaCl droplets using both the standard ICRP hygroscopic response and the semi-analytic kinetic model is shown in figure 2B. Differences between

the ICRP treatment using the conventional hygroscopic response and the refined treatment are apparent, regardless of the RH in which the aerosol is equilibrated or the initial size. The difference in this size region greater than 50 μm is largely unimportant as the deposition of aerosols within this size regime tends to be 100% of the inhalable fraction.

2.3 Conditions of the Model

All parameters used for the model, aside from the specific diameter growth factor/water activity relationships for the aerosol considered here, have been described in detail previously.[32] Unless otherwise stated, the conditions were those for a healthy Caucasian male breathing through his nose while doing light exercise with an RH within the lung of 99%. The RH in the lung of a healthy individual has been estimated to reach near saturation with an RH between 99% and 99.5%.[48, 49] The simulations from the model developed here are identified in the figures by the ambient RH immediately prior to inhalation. The simulations produced using the traditional ICRP model are identified by the $d_{ae}(\infty)$ value (Eq. 4).

Note that not all particle growth occurring during inhalation may be steady; rather rapid non-linear size changes of crystalline aerosol particles are known to occur through deliquescence (e.g. RH of 75% for NaCl) during inhalation. This would result in inhaled dry NaCl particles undergoing no growth in the upper airways followed by rapid growth in the deep lung. To simplify the model, all aerosol is maintained as a liquid, where the solute concentration ranged from dilute, to saturated, through to supersaturated (between 50% RH and 75% for NaCl). Salt particles are only modelled down to an RH of 50% while organic aerosol are modelled down to RH <20 %.

3.0 Results

3.1 Validation of model through comparison with experimental data

Two commonly referenced studies that examined the deposition of mono-disperse aerosol in the respiratory tract were reported by Tu and Knutson,[50] and by Blanchard and Willeke.[51] The structure of these studies was as follows: NaCl[50, 51] (or kerosene [50]) was nebulized, dried, size selected and held in a Teflon bag. Immediately prior to inhalation, Tu and Knutson raised the RH of the droplets to 95%, while Blanchard and Willeke left the aerosol dry. The difference in aerosol counts between the inhaled and exhaled air was then measured. The results of their studies are shown in figure 3.

All of the parameters and experimental conditions used by Tu and Knutson, from the generation of the aerosol, to the pre-treatment and biological factors such as lung volume and sex, are able to be accounted for in the model developed here and a comparison is shown in figure 3. Excellent

agreement was found for both the hygroscopic (NaCl) and hydrophobic (kerosene) aerosols. Proper consideration of the pre-treatment of the NaCl aerosol prior to inhalation was essential to accurately predict the deposition pattern (figure 3A).

The importance of quantifying the hygroscopicity of the aerosol is shown in figure 3B. Kerosene is a hydrocarbon liquid consisting of a mixture of carbon chains between 6 and 16 carbon per molecule. The κ value of a low solubility organic aerosol is ~0.03[52] . Excellent agreement in total dose between the model and experimental results is observed only if the aerosol is assumed to have low hygroscopicity with values between 0.05 and 0.01. This demonstrates that through accurately simulating the dynamics of organic aerosol growth, accurate predictions of aerosol deposition within the lung are possible in the ICRP framework.

3.2 The ambient RH affects the deposition pattern of pure inorganic aerosol

The influence of the RH prior to inhalation on the deposition pattern of NaCl within the lung is shown in figure 4A. Of particular interest in this study is how specific changes in the model conditions affected the deposition pattern. For ease of comparison between multiple deposition patterns, rather than reporting multiple full deposition patterns, we report the differences in the deposition fractions for two different environments. In doing this, the subtle changes in the deposition pattern become immediately apparent (figure 4B). For particles larger than 0.1 μm in diameter, lowering the RH prior to inhalation was found to lead to a significant increase in lung deposition in every region, with the largest increases observed in the alveolar-interstitial region and, to a slightly lesser extent, in the bronchial region. Deposition in this size regime is governed by aerosol impaction and sedimentation, suggesting that increasing the magnitude of the size change of particles during inhalation increases the influence of these deposition mechanisms. Below 0.1 μm, lowering the RH prior to inhalation has the opposite effect, slightly lowering the aerosol deposition in the bronchi and alveolar regions. The reason for this reduction in deposition fraction is attributed to the increase in aerodynamic diameter for the aerosol particles following inhalation: the particles become too large to be removed via diffusion while remaining too small to be removed via sedimentation.

Similar comparisons of the deposition pattern of NaCl aerosols, as predicted by the standard ICRP model (with $d_{ae}(\infty) = 3$) and for NaCl aerosol at an ambient RH of 50% (as predicted by our model) are shown in figure 4C. For aerosol larger than 100 nm, a similar deposition pattern was observed for these two simulations; this was not unexpected given that the ICRP model used with a $d_{ae}(\infty) = 3$ is commonly used to predict total and regional dose of NaCl.

When the ambient RH is increased to 90% (figure 4D), a more pronounced difference between the traditional ICRP estimation and the refined model is observed in the deposition pattern. Below 100 nm, the ICRP underestimates the overall deposition by ~20% due to an overestimation in the magnitude of water uptake when the surface curvature (or Kelvin effect) is not considered (figure 2B). The importance of the Kelvin effect in aerosol dynamics is well understood, hence its integration in numerous lung deposition models.[53, 54] The absence of an appreciation of the Kelvin effect in the standard ICRP model limits its accuracy for predicting aerosol deposition for this size region. Figure 4D clearly demonstrates the limitations of the standard ICRP model: ambient conditions are not considered which leads to inaccurate estimations of dose.

Due to the insensitivity of the radial growth dependence of aerosol on RH over the ambient temperature range 0 – 40 ^{O}C, changing the ambient temperature was found to have no effect on the deposition pattern (data not shown).

The effect of aerosol hygroscopicity on the deposition pattern for aerosol containing similar species was examined. NaCl and ammonium sulphate ($(NH_4)_2SO_4$) both have well-defined deliquescence (75% for NaCl and 79% for $(NH_4)_2SO_4$) and efflorescence (45% for NaCl and 37% for $(NH_4)_2SO_4$) RHs, but show subtle differences in their radial growth factors when the aerosol is liquid (Supplemental Figure 1A). Despite NaCl and $(NH_4)_2SO_4$ having similar hygroscopic behaviour, a significant difference in the deposition pattern in the lung was observed in their inhalation simulations (Supplemental Figure 2); the largest difference, of 14%, between the two deposition patterns was for aerosol with a diameter around 700 nm.

3.3 The RH in the lung affects the deposition pattern of pure NaCl aerosol

The RH within the alveolar regions of the lung is considered to be near saturation (~99.5%).[55] In the upper airways, the RH is dependent on many factors including the RH of the inhaled air, breathing rate and the disease state of the individual. RH probes are notoriously inaccurate at RH above 90% with a typical error associated with the probe in excess of ±2%, thus making direct and reliable measurements of the RH in the upper airway impossible. The sensitivity of the deposition pattern of NaCl aerosol to the assumed humidity within the lung is significant (figure 5 and Supporting Information Figure 3), with upwards of 45% more aerosol ranging in size between 800 to 900 nm being deposited in the healthy lung that the diseased lung (figure 5A).

3.4 The physicochemical properties of organic aerosol affect the lung deposition pattern

Organic aerosols are common to urban environments. Of interest to this study are the differences in the deposition pattern in the lung resulting from changes to the physicochemical of the organic aerosol (figure 6).

A reduction in the hygroscopicity parameter κ (see Eq. 6) leads to significant changes in both the rate and magnitude of the size change of the aerosol during inhalation across a broad range of initial diameters (figure 6A). This difference in size leads to a significant change in the deposition pattern in the lung (figure 6B and Supporting Figure 4).

Common to organic aerosols is the presence of surface active species that can limit the rate of mass flux to and from the droplet. In modelling aerosol mass flux, the likelihood of water uptake is characterised by the mass accommodation coefficient (α), which is equivalent to the fraction of molecular collisions of water with the surface that lead to absorption within the aerosol droplet bulk. For pure water, α is above 0.5[56] and is reduced as the surface of the droplet becomes covered with surface active species.[35] The sensitivity of the deposition pattern to the mass accommodation coefficient was explored (figure 6C). Minimal differences in the deposition pattern were observed until α was reduced to 5×10^{-4}. For reference, this α value is similar to that for the evaporation coefficient for water transport across the interface of a drying aerosol droplet coated in 1-pentadecanol ($C_{15}H_{31}OH$).

3.5 Estimating regional and total dose of indoor air pollution as a function of relative humidity

Regardless of aerosol type, the majority of fluctuations in regional and total dose as a function of ambient RH were observed for aerosol between 100 nm and 10 μm. The sources of indoor particulate air pollution are limited, resulting in a size regime encapsulated in this region (centred ~1 μm in diameter[57]). Based on the size distribution of indoor particulate air pollution measured by Yang *et al.* (Supporting Figure 6),[57] the changes in regional and total dose were estimated using the modified ICRP model (figure 7).

Ambient RH was found to have little effect on the total dose (figure 7D), or the dose delivered to the exothoracic region (figure 7A). However, the hygroscopic response was shown to shift significantly deposition to the alveolar region from the bronchiolar region as the ambient RH increased.

Ambient RH may affect the adverse health effects associated with indoor air pollution (figure 7). The location in the lung that the dose is delivered will be affected by ambient RH, which may have a dramatic effect on the downstream biological response. The potential for adverse health effects

287 associated with these shifts in deposition pattern to result from long term exposure will need to be
288 explored further.

289

290 **4.0 Discussion**

291 A novel adaptation to the traditional ICRP model to incorporate a detailed treatment of the kinetic and
292 thermodynamic response of the aerosol during inhalation is presented. The parameters of the model
293 are presented (Tables 1 and SI1). This model can readily predict the total and regional dose for any
294 aerosol where the hygroscopic growth as a function of RH is known; for numerous pure (and
295 multicomponent) aerosols, there are many aerosol thermodynamic models to predict this behaviour
296 available online (e.g. the Extended AIM Aerosol Thermodynamics Model).

297 The condensational growth of a droplet during inhalation is governed both by the hygroscopic
298 capacity of a droplet to grow (a thermodynamic factor) and the kinetics of mass fluxes. Although the
299 largest changes in the deposition pattern results when the capacity for hygroscopic growth is
300 accurately accounted for, kinetic factors do also play an important role with size changes occurring on
301 the same timescale as inhalation/exhalation, particularly if precise estimations of regional and total
302 dose are required (figure 6C).

303 A common observation seen here is that changes to aerosol growth, whether due to the aerosol
304 composition or the RH (either in the lung or ambient), affect the deposition fraction in opposing ways
305 for particles smaller and larger than 100 nm. For example, consider the effect of RH within the lung
306 itself on regional dose. The airway with an RH of 95% (figure 5A) experiences a substantial decrease
307 in the overall aerosol deposition in the size region between 0.1 and 5 μm when compared to the
308 healthy lung while at the same time an increase in total aerosol deposition for aerosol under 100 nm
309 was predicted for the lung with an RH of 95%. Broadly speaking, limitations to aerosol growth lead
310 to an increase in the deposition frequency of aerosol under 100 nm, and a decrease in the deposition
311 frequency of the aerosol between 0.1 and 10 μm. Thus, the consequences of hygroscopic growth
312 during inhalation on the deposition pattern is dependent on aerosol size (whether it is above or below
313 100 nm) and should be treated as such.[58]

314 The importance of the hygroscopic behaviour of inhaled aerosol on the deposition pattern may be
315 amplified for those with diseases of the lung. For example, asthmatics experience airway constriction
316 and difficulty breathing in humid conditions, which is believed to be triggered by airway sensory
317 nerves that are sensitive to temperature changes.[59] Additionally, the inhalation of submicron
318 particulates also triggers similar asthmatic symptoms.[60] In section 3.2, aerosol particles under 100 nm
319 in diameter were shown to deposit to a higher degree when the aerosol growth during inhalation was

limited at higher ambient RH (figure 4B). Thus, limitations to aerosol growth during inhalation could lead to a larger dose of sub 100 nm in diameter aerosol particles penetrating deep into the lung and may trigger and amplify asthmatic symptoms.

The results of figure 5 may be used to gain insight into both the pathogenesis and treatment of lung diseases such as asthma and chronic obstructive pulmonary disease (COPD), where both conditions result from chronic inflammation and are characterized by airway wall thickening.[61, 62] The thickening of the airway wall leads to an overall reduction of the humidity within the afflicted lungs.[63] Both the exacerbation and pathogenesis of these conditions have been associated with the inhalation of particulate air pollution with an aerodynamic diameter under 100 nm. As shown in figure 7, a reduction of humidity in the lung leads to an increase in the deposition of aerosols within this size fraction deep in the lung. In the treatment of asthma and COPD, the drug is delivered directly to the lung through the inhalation of a pharmaceutical-containing aerosol. The aerosols generated from pharmaceutical delivery devices (e.g. nebulizers) typically have a log-normal particle size distribution with a mean aerodynamic diameter between 3 and 5 μm. When compared to the humid lung (RH of 99.9%), the dry lung (RH of 95%) shows a reduction in pharmaceutical aerosol deposition, meaning the effective dose of these pharmaceutics may be reduced by up to 50%. There is increasing evidence that drug deposition into the peripheral lung provides an improved clinical treatment compared to large aerosol treatment.[64] This reduction in dose to the deep lung has the potential to reduce in drug efficacy; further study is required to explore this further. It should be noted that airway remodelling (e.g. gland enlargement, subepithelial fibrosis, epithelial alterations) can be a common feature of some diseases of the lung, such as emphysema and COPD.[65] These modifications (e.g. breakdown of tissue, mucus-hypersecretion) will clearly have a significant effect on the aerosol deposition rate in the lung as narrower airways will lead to a higher deposition rate via diffusion (remembering that deposition via diffusion is a function of aerosol diameter/hygroscopic growth). An improved understanding of the interplay between aerosol dynamics and the physical structure of the lung and their combined influence on deposition rates is critical for studying both the treatment, and pathogenesis, of lung disease.

Although there is an appreciation of the hygroscopic growth of an aerosol during inhalation on total and regional dose, what is continually overlooked are the conditions of the aerosol prior to inhalation, specifically the RH in which it is situated. An example of this is the article by Mitsakou *et al*.[54] where they developed a whole lung Eulerian model to predict aerosol deposition. In the model, aerosol growth is calculated using the theory described by Mason;[66] the humidity in which the aerosol originates is not considered and the aerosol growth calculated is that of an originally dry aerosol. This oversight meant that the aerosol growth in their model may be overestimated, which may explain the slight (~5-10%) over estimation in the deposition fraction observed when their model was compared

355 to experimental data; over estimating aerosol growth leads to an increase in the deposition fraction for
356 aerosol 0.01 to 1 μm in diameter (figure 4). The sensitivity to the ambient RH is typically not
357 considered in lung inhalation models; in the literature review made during the preparation of this
358 manuscript, no articles discussing this point were found. We speculate that this oversight is present in
359 numerous models, and consideration of it should serve to improve other current inhalation models.

360

361 **5.0 Acknowledgments**

362 We thank the Elizabeth Blackwell Institute (EBI) and the Wellcome Trust Institutional Strategic
363 Support Fund to the University of Bristol for financial support through the EBI Early Career Research
364 Fellowship awarded to AEH, and the EPSRC for financial support through a Leadership Fellowship
365 awarded to JPR (grant reference EP/G007713/1).

366 Supporting Information is available free of charge via the Internet at http://pubs.acs.org. The table
367 and figures include data input in the model (e.g. core equations used to produce the model, radial
368 growth curves, size distributions), and model predictions of regional and total dose as a function of
369 various parameters (e.g. aerosol composition, lung conditions).

370

6.0 Figures

Figure 1

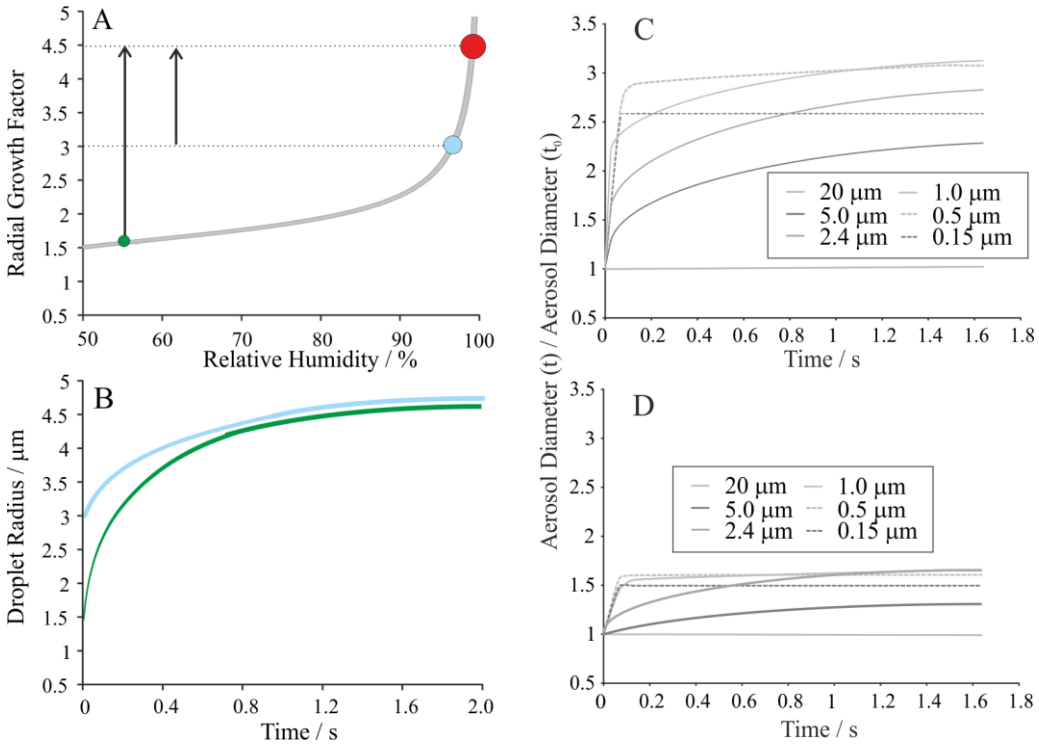

The (A) relative magnitude and (B) absolute rate of hygroscopic growth of a single inhaled NaCl aerosol droplet when the ambient RH prior to inhalation is at 55% (green) and 95% (blue); the dry radius for both particles is 1 µm. The arrows in (A) show the magnitude of change in radial growth factor (indicated by the dotted lines) two droplets will experience during inhalation; the droplet initially suspended in air at RH=55% will grow more than the droplet initially suspended at an RH=95% during inhalation. The relative growth following inhalation of NaCl aerosols of various initial diameters that have equilibrated at RHs of (C) 50% and (D) 95%.

Figure 2

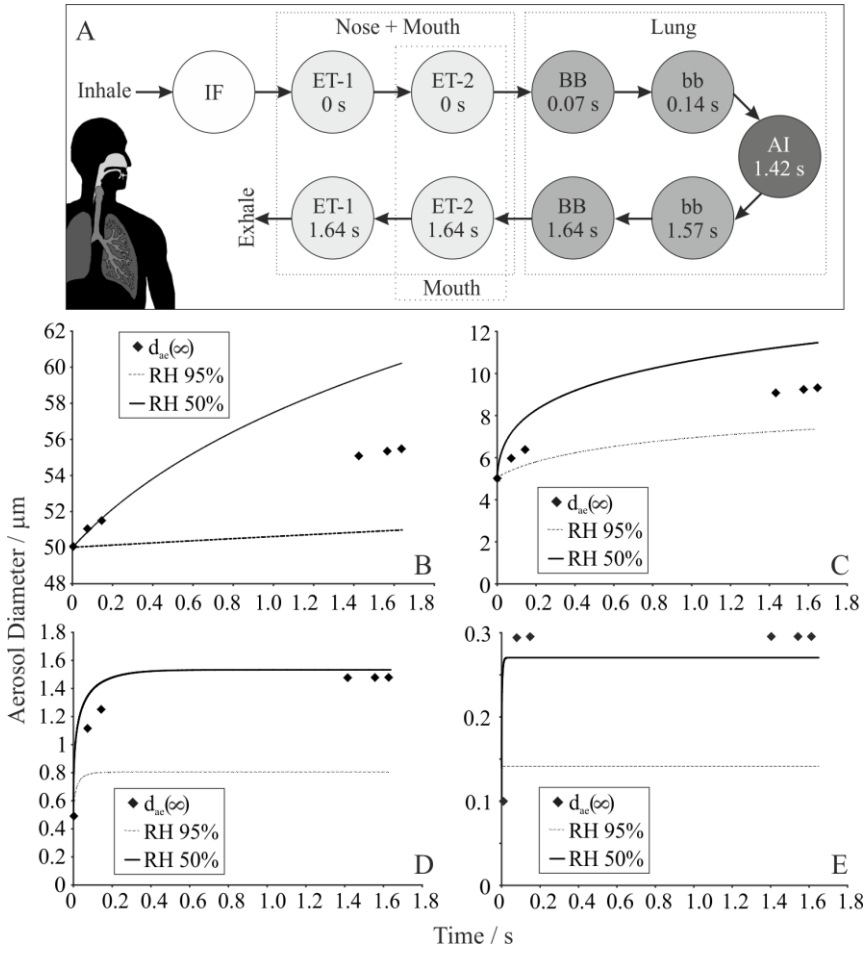

(A): The structure of the ICRP model (see text for definitions of regions); each anatomical region of the lung is indicated by shade for both the inset image and circles. The time point in which the parcel of air passes through each given region is indicated by number within each circle. The hygroscopic growth of aerosols of initial diameters of (B) 50 µm, (C) 5 µm, (D) 0.5 µm and (E) 0.05 µm following inhalation where the RH within the lung is 99% as predicted by the ICRP model ($d_{ae}(\infty)$ = 3.0) (diamonds) and by the semi-analytical solution to the mass and heat flux equations of Kulmala *et al* [39] (lines) (where the ambient RH was either 50% or 95%). Note that the time points indicated in the circles of (A) correspond with those for $d_{ae}(\infty)$ in (B).

Figure 3

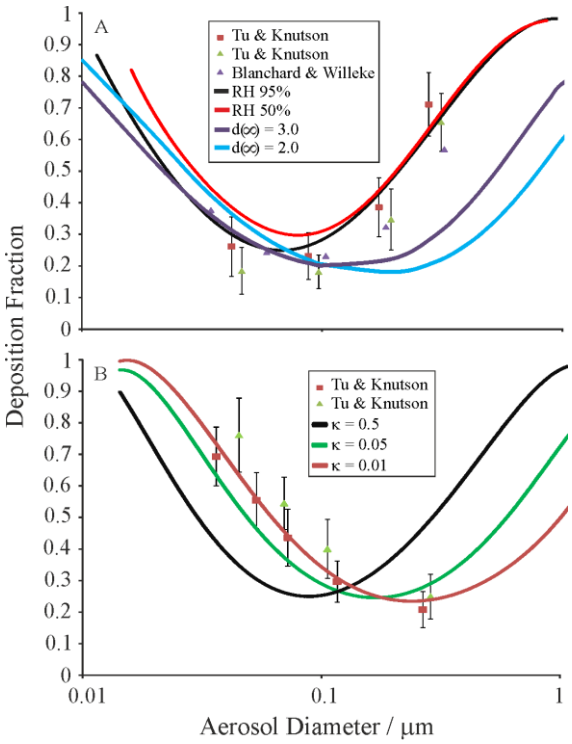

Comparison of the deposition fraction of (A) NaCl and (B) organic aerosol mimics in the lung predicted by the model developed here and the traditional ICRP model with the experimental data collected by Tu & Knutson [50] and Blanchard & Willeke.[51] For both (A) and (B), the symbols indicate previously reported experimental data of human exposure. For (A), the lines indicate dose predictions from the traditional ICRP model (d(∞)=3.0 and d(∞)=2.0) and from the adapted ICRP model reported here (where the ambient RH was either 50% or 95%). For (B), the lines indicate dose predictions from only the adapted ICRP model reported here while the hygroscopic behaviour of the aerosol was estimated by setting the κ-value given into equation 6 (Supplementary Information Figure S-1).

Figure 4

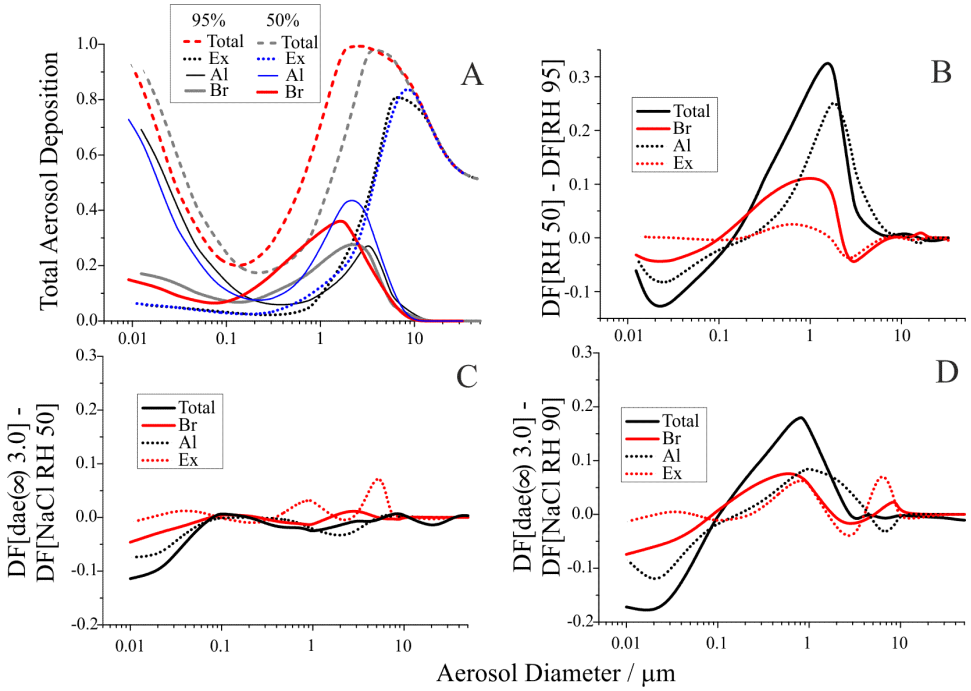

(A) Deposition fraction (DF) of NaCl aerosols in the extrathoracic region (Ex), bronchial region (Br), alveolar-interstitial region (Al) and total lung (Total) as a function of relative humidity (RH) the aerosol experiences prior to inhalation. Differences in the DF of inhaled aerosol as a function of the magnitude of aerosol growth during inhalation are also reported. Specifically, changes in the DF of NaCl aerosols resulting from the conditions of the aerosol immediately prior to inhalation are explored. (B) is the difference in deposition fraction for NaCl suspended in an ambient air with an RH of 50% and 95% prior to inhalation. The difference in deposition fraction between the ICRP model prediction of hydrophilic aerosol and the prediction for NaCl suspended in an ambient air with an RH of (C) 50% and (D) 95% prior to inhalation.

Figure 5

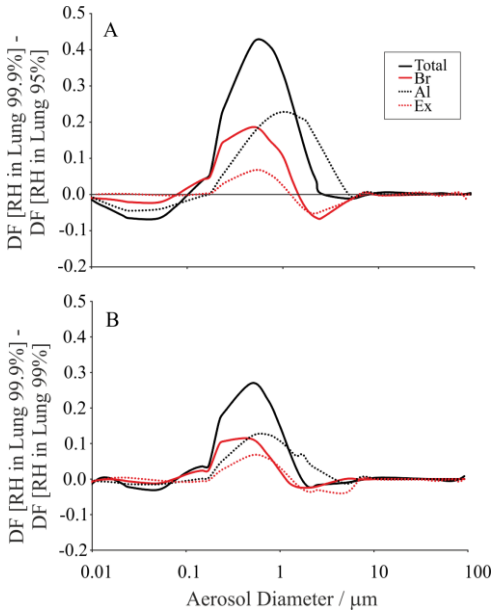

Differences in the deposition fraction (DF) of inhaled aerosol (initially at an ambient RH of 50%) resulting from the changes in RH in the lung as a function of aerosol diameter. Deposition in a lung with an RH of 99.9% is compared with deposition in a lung with an RH of (A) 95% and (B) 99%. Total deposition (Total), combined bronchi and bronchiolar (Br), extrathoracic (nose, mouth and throat) (Ex), and alveolar-interstitial (Al).

Figure 6

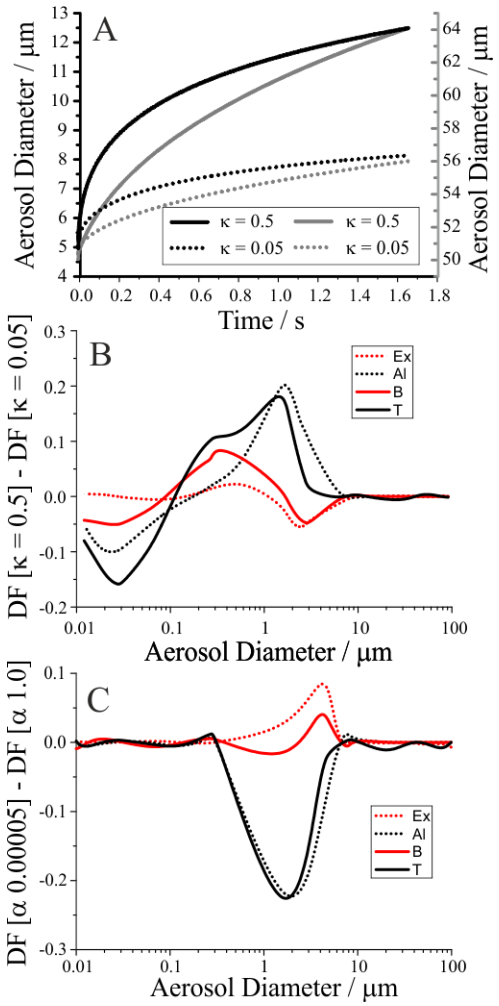

How the growth dynamics of organic aerosol affect total and regional dose. (A) The growth kinetics of two organic aerosols of different hydrophobicities in the lung where the ambient RH is 20%. The colour of the line indicates the starting diameter of the droplet (black for 5 micrometers, left y-axis. And grey for 50 micrometers, right axis) while the line style indicates hygroscopicity of the droplet (i.e. the value of κ). (B) How this difference in dynamic behaviour of the aerosol described in (A) will affect the subsequent deposition fraction (DF) of the aerosol in the lung. (C) Surface active species affect the total and regional doses; the deposition pattern of organic aerosol with a mass accommodation coefficient (α) of 0.00005 is compared to that of water. Total deposition (T), combined bronchi and bronchiolar (B), extrathoracic (nose, mouth and throat) (Ex), and alveolar-interstitial (Al).

Figure 7

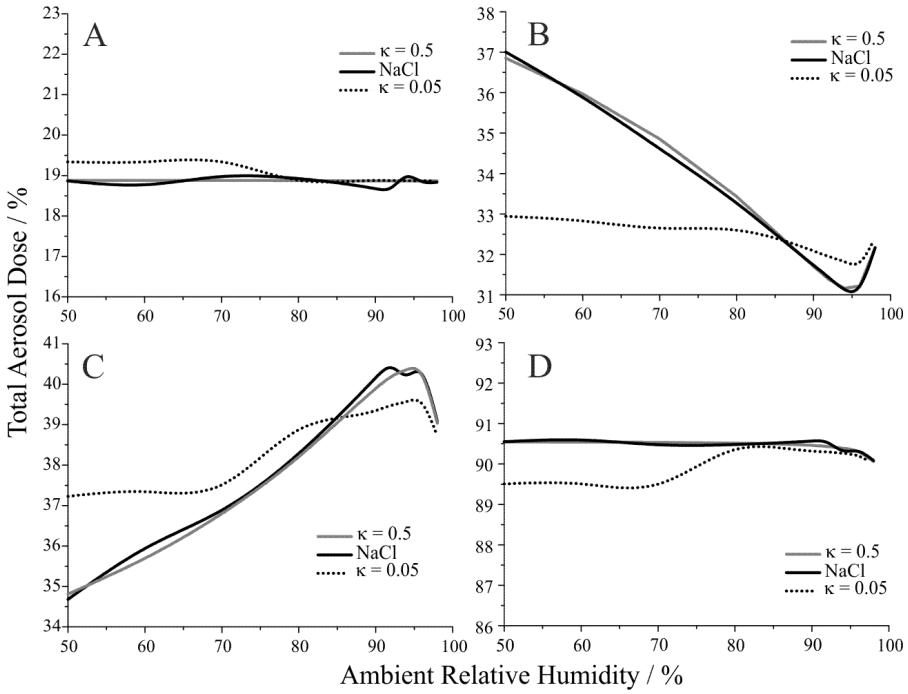

The percentage of the total dose of indoor particulate air pollution delivered to the exothoracic region (A), bronchi region (B), alveolar region (C) and the whole (D) lung as a function of ambient RH and particle type. The specific particle types shown consist of a solute of either pure NaCl or an organic aerosol mimic for which the hygroscopic behaviour is determined by the value of κ (equation 6), with a value of 0.5 representing a hygroscopic aerosol and a value of 0.05 an aerosol of low hygroscopic response. Doses were modelled for a male at rest breathing through his mouth.

7.0 Tables

Table 1: Variables Used in Modified ICRP Model

Symbol	Unit	Name and/or Meaning
d_{ae}	μm	Aerodynamic diameter
$d_{ae}(0)$	μm	Aerodynamic diameter at the point of inhalation
$d_{ae}(t)$	μm	Aerodynamic diameter at time *t*
$d_{ae}(\infty)$	Unitless	Equilibrium growth value/Relative growth in the lung the aerosol will reach given an infinite amount of time
t	s	Time from the point aerosol enters respiratory tract
I	g/s	Instantaneous mass fulx to or from a droplet
a	μm	Droplet radius
S_∞	Unitless	Water saturation ratio in the gas phase of the aerosol
β_m	Unitless	Transitional correction factors for mass
βT	Unitless	Transitional correction factors for temperature
a_w	Unitless	Activity of water at the surface of the droplet
M	g/mol	Molar mass of water
D_w	cm^2/s	Diffusion coefficient of water in the gas phase
$p_{v,\infty}$	Pa	Saturation vapour pressure of water
A	Unitless	Stefan flow correction
K	W/(mK)	Thermal conductivity of the gas phase
R	$m^3PaK^{-1}mol^{-1}$	Molar gas constant
L	J/kg	Latent heat of vaporization per unit weight of water
Sh	Unitless	Sherwood number/ Accounts for the enhancement of mass flux in an airflow
GF	Unitless	Radial growth factor
κ	Unitless	Dimensionless hygroscopicity parameter from κ-Kohler theory
S_a	Unitless	Activity at the surface of the droplet
T_∞	K	Gas temperature
D	cm^2/s	Diffusion coefficient of aerosol

8.0 References

1. Pope, C. A.; Thun, M. J.; Namboodiri, M. M.; Dockery, D. W.; Evans, J. S.; Speizer, F. E.; Heath, C. W., Particulate Air-Pollution as a Predictor of Mortality in a Prospective-Study of Us Adults. *Am. J. Respir. Crit. Care Med.* **1995,** *151*, (3), 669-674.
2. Pope, C. A.; Ezzati, M.; Dockery, D. W., Fine-Particulate Air Pollution and Life Expectancy in the United States. *New Engl J Med* **2009,** *360*, (4), 376-386.
3. Araujo, J. A.; Nel, A. E., Particulate matter and atherosclerosis: role of particle size, composition and oxidative stress. *Part Fibre Toxicol* **2009,** *6*, (24), 1-19.
4. Anderson, J. O.; Thundiyil, J. G.; Stolbach, A., Clearing the air: a review of the effects of particulate matter air pollution on human health. *J. Med. Toxicol.* **2012,** *8*, (2), 166-75.
5. Hofmann, W., Modelling inhaled particle deposition in the human lung-A review. *J Aerosol Sci* **2011,** *42*, (10), 693-724.
6. Rostami, A. A., Computational modeling of aerosol deposition in respiratory tract: a review. *Inhal Toxicol* **2009,** *21*, (4), 262-90.
7. Yeh, H. C.; Schum, G. M., Models of human lung airways and their application to inhaled particle deposition. *Bull Math Biol* **1980,** *42*, (3), 461-80.
8. Butler, J. P.; Tsuda, A., Effect of convective stretching and folding on aerosol mixing deep in the lung, assessed by approximate entropy. *J Appl Physiol* **1997,** *83*, (3), 800-9.
9. Finlay, W. H.; Smaldone, G. C., Hygroscopic behavior of nebulized aerosols: Not as important as we thought? *J Aerosol Med* **1998,** *11*, (4), 193-195.
10. Finlay, W. H., Estimating the type of hygroscopic behavior exhibited by aqueous droplets. *J Aerosol Med* **1998,** *11*, (4), 221-9.
11. Davies, J. F.; Haddrell, A. E.; Reid, J. P., Time-Resolved Measurements of the Evaporation of Volatile Components from Single Aerosol Droplets. *Aerosol Sci Tech* **2012,** *46*, (6), 666-677.
12. Chan, C. K.; Liang, Z.; Zheng, J. A.; Clegg, S. L.; Brimblecombe, P., Thermodynamic properties of aqueous aerosols to high supersaturation .1. Measurements of water activity of the system Na+-Cl--NO3--SO42--H2O at similar to 298.15 K. *Aerosol Sci Tech* **1997,** *27*, (3), 324-344.
13. Clegg, S. L.; Seinfeld, J. H.; Brimblecombe, P., Thermodynamic modelling of aqueous aerosols containing electrolytes and dissolved organic compounds. *J Aerosol Sci* **2001,** *32*, (6), 713-738.
14. Davies, J. F.; Haddrell, A. E.; Miles, R. E.; Bull, C. R.; Reid, J. P., Bulk, surface, and gas-phase limited water transport in aerosol. *J Phys Chem A* **2012,** *116*, (45), 10987-98.
15. Broday, D. M.; Georgopoulos, P. G., Growth and deposition of hygroscopic particulate matter in the human lungs. *Aerosol Sci Tech* **2001,** *34*, (1), 144-159.
16. Khajeh-Hosseini-Dalasm, N.; Longest, P. W., Deposition of particles in the alveolar airways: Inhalation and breath-hold with pharmaceutical aerosols. *J Aerosol Sci* **2015,** *79*, 15-30.
17. Winkler-Heil, R.; Ferron, G.; Hofmann, W., Calculation of hygroscopic particle deposition in the human lung. *Inhal Toxicol* **2014,** *26*, (3), 193-206.
18. Conway, J., Lung imaging - two dimensional gamma scintigraphy, SPECT, CT and PET. *Adv Drug Deliv Rev* **2012,** *64*, (4), 357-68.
19. Fleming, J.; Conway, J.; Majoral, C.; Bennett, M.; Caillibotte, G.; Montesantos, S.; Katz, I., A Technique for Determination of Lung Outline and Regional Lung Air Volume Distribution from Computed Tomography. *J Aerosol Med* **2013,** *27(1)*, 35-42.
20. Longest, P. W.; Hindle, M., CFD simulations of enhanced condensational growth (ECG) applied to respiratory drug delivery with comparisons to in vitro data. *J Aerosol Sci* **2010,** *41*, (8), 805-820.
21. Hindle, M.; Longest, P. W., Evaluation of Enhanced Condensational Growth (ECG) for Controlled Respiratory Drug Delivery in a Mouth-Throat and Upper Tracheobronchial Model. *Pharm. Res.* **2010,** *27*, (9), 1800-1811.
22. Byron, P. R.; Hindle, M.; Lange, C. F.; Longest, P. W.; McRobbie, D.; Oldham, M. J.; Olsson, B.; Thiel, C. G.; Wachtel, H.; Finlay, W. H., In Vivo-In Vitro Correlations: Predicting Pulmonary Drug Deposition from Pharmaceutical Aerosols. *J. Aerosol Med. Pulm. Drug Deliv.* **2010,** *23*, S59-S69.

23. Grgic, B.; Martin, A. R.; Finlay, W. H., The effect of unsteady flow rate increase on in vitro mouth-throat deposition of inhaled boluses. *J Aerosol Sci* **2006,** *37*, (10), 1222-1233.
24. Holbrook, L. T.; Longest, P. W., Validating CFD predictions of highly localized aerosol deposition in airway models: In vitro data and effects of surface properties. *J Aerosol Sci* **2013,** *59*, 6-21.
25. Camner, P.; Anderson, M.; Philipson, K.; Bailey, A.; Hashish, A.; Jarvis, N.; Bailey, M.; Svartengren, M., Human bronchiolar deposition and retention of 6-, 8- and 10-micrograms particles. *Exp Lung Res* **1997,** *23*, (6), 517-35.
26. Davesne, E.; Paquet, F.; Ansoborlo, E.; Blanchardon, E., Absorption of plutonium compounds in the respiratory tract. *J Radiol Prot* **2010,** *30*, (1), 5-21.
27. Bair, W. J., The Icrp Human Respiratory-Tract Model for Radiological Protection. *Radiat Prot Dosim* **1995,** *60*, (4), 307-310.
28. Bair, W. J., The Revised International Commission on Radiological Protection (Icrp) Dosimetric Model for the Human Respiratory Tract - an Overview. *Inhaled Particles Vii* **1994**, 251-256.
29. Huston, T. E.; Farfan, E. B.; Bolch, W. E.; Bolch, W. E., Influences of parameter uncertainties within the ICRP-66 respiratory tract model: A parameter sensitivity analysis. *Health Phys* **2003,** *85*, (5), 553-566.
30. Farfan, E. B.; Huston, T. E.; Bolch, W. E.; Han, E.; Beharry, K.; Jupiter, K., Influence of age, gender, and exertion level on dose uncertainties associated with inhalation of weapons-grade plutonium oxide. *Health Phys* **2003,** *84*, (6), S171-S171.
31. Bolch, W. E.; Huston, T. E.; Farfan, E. B.; Vernetson, W. G.; Bolch, W. E., Influences of parameter uncertainties within the ICRP-66 respiratory tract model: Particle clearance. *Health Phys* **2003,** *84*, (4), 421-435.
32. Yu, K. N.; Lau, B. M. F.; Nikezic, D., Assessment of environmental radon hazard using human respiratory tract models. *J Hazard Mater* **2006,** *132*, (1), 98-110.
33. Human respiratory tract model for radiological protection. A report of a Task Group of the International Commission on Radiological Protection. *Annals of the ICRP* **1994,** *24*, (1-3), 1-482.
34. Londahl, J.; Massling, A.; Swietlicki, E.; Brauner, E. V.; Ketzel, M.; Pagels, J.; Loft, S., Experimentally Determined Human Respiratory Tract Deposition of Airborne Particles at a Busy Street. *Environ. Sci. Technol.* **2009,** *43*, (13), 4659-4664.
35. Davies, J. F.; Miles, R. E. H.; Haddrell, A. E.; Reid, J. P., Influence of organic films on the evaporation and condensation of water in aerosol. *P Natl Acad Sci USA* **2013,** *110*, (22), 8807-8812.
36. Davies, J. F.; Haddrell, A. E.; Rickards, A. M. J.; Reid, J. P., Simultaneous Analysis of the Equilibrium Hygroscopicity and Water Transport Kinetics of Liquid Aerosol. *Anal Chem* **2013,** *85*, (12), 5819-5826.
37. Haddrell, A. E.; Hargreaves, G.; Davies, J. F.; Reid, J. P., Control over hygroscopic growth of saline aqueous aerosol using Pluronic polymer additives. *Int J Pharm* **2013,** *443*, (1-2), 183-192.
38. Haddrell, A. E.; Davies, J. F.; Miles, R. E. H.; Reid, J. P.; Dailey, L. A.; Murnane, D., Dynamics of aerosol size during inhalation: Hygroscopic growth of commercial nebulizer formulations. *Int. J. Pharm.* **2014,** *463*, (1), 50-61.
39. Kulmala, M.; Vesala, T.; Wagner, P. E., An Analytical Expression For the Rate of Binary Condensational Particle Growth. *Proc R Soc A* **1993,** *441*, (1913), 589-605.
40. Bones, D. L.; Reid, J. P.; Lienhard, D. M.; Krieger, U. K., Comparing the mechanism of water condensation and evaporation in glassy aerosol. *P Natl Acad Sci USA* **2012,** *109*, (29), 11613-11618.
41. Miles, R. E. H.; Knox, K. J.; Reid, J. P.; Laurain, A. M. C.; Mitchem, L., Measurements of Mass and Heat Transfer at a Liquid Water Surface during Condensation or Evaporation of a Subnanometer Thickness Layer of Water. *Phys Rev Lett* **2010,** *105*, (11), 116101(1)-116101(4).
42. Topping, D. O.; McFiggans, G. B.; Coe, H., A curved multi-component aerosol hygroscopicity model framework: Part 1 - Inorganic compounds. *Atmos Chem Phys* **2005,** *5*, 1205-1222.
43. Topping, D. O.; McFiggans, G. B.; Coe, H., A curved multi-component aerosol hygroscopicity model framework: Part 2 - Including organic compounds. *Atmos Chem Phys* **2005,** *5*, 1223-1242.

552 44. Petters, M. D.; Kreidenweis, S. M., A single parameter representation of hygroscopic growth
553 and cloud condensation nucleus activity. *Atmos Chem Phys* **2007,** *7*, (8), 1961-1971.
554 45. Zdanovskii, A. B., Novyi Metod Rascheta Rastvorimostei Elektrolitov V
555 Mnogokomponentnykh Sistemakh .2. *Zh Fiz Khim+* **1948,** *22*, (12), 1486-1495.
556 46. Zdanovskii, A. B., Novyi Metod Rascheta Rastvorimostei Elektrolitov V
557 Mnogokomponentnykh Sistemakh .1. *Zh Fiz Khim+* **1948,** *22*, (12), 1478-1485.
558 47. Stokes, R. H.; Robinson, R. A., Interactions in Aqueous Nonelectrolyte Solutions .I. Solute-
559 Solvent Equilibria. *J Phys Chem-Us* **1966,** *70*, (7), 2126-&.
560 48. Ferron, G. A.; Haider, B.; Kreyling, W. G., A Method for the Approximation of the Relative-
561 Humidity in the Upper Human Airways. *Bull. Math. Biol.* **1985,** *47*, (4), 565-589.
562 49. Cothern, C. R.; Smith, J. E., *Environmental radon*. Plenum Press: New York, 1987; p xiii,
563 363 p.
564 50. Tu, K. W.; Knutson, E. O., Total Deposition of Ultrafine Hydrophobic and Hygroscopic
565 Aerosols in the Human Respiratory System. *Aerosol Sci Tech* **1984,** *3*, (4), 453-465.
566 51. Blanchard, J. D.; Willeke, K., Total deposition of ultrafine sodium chloride particles in human
567 lungs. *J Appl Physiol* **1984,** *57*, (6), 1850-6.
568 52. Carrico, C. M.; Petters, M. D.; Kreidenweis, S. M.; Sullivan, A. P.; McMeeking, G. R.; Levin,
569 E. J. T.; Engling, G.; Malm, W. C.; Collett, J. L., Water uptake and chemical composition of fresh
570 aerosols generated in open burning of biomass. *Atmos Chem Phys* **2010,** *10*, (11), 5165-5178.
571 53. Kleinstreuer, C.; Feng, Y., Lung Deposition Analyses of Inhaled Toxic Aerosols in
572 Conventional and Less Harmful Cigarette Smoke: A Review. *Int J Env Res Pub He* **2013,** *10*, (9),
573 4454-4485.
574 54. Mitsakou, C.; Helmis, C.; Housiadas, C., Eulerian modelling of lung deposition with sectional
575 representation of aerosol dynamics. *J Aerosol Sci* **2005,** *36*, (1), 75-94.
576 55. Labiris, N. R.; Dolovich, M. B., Pulmonary drug delivery. Part I: Physiological factors
577 affecting therapeutic effectiveness of aerosolized medications. *Brit J Clin Pharmaco* **2003,** *56*, (6),
578 588-599.
579 56. Miles, R. E. H.; Reid, J. P.; Riipinen, I., Comparison of Approaches for Measuring the Mass
580 Accommodation Coefficient for the Condensation of Water and Sensitivities to Uncertainties in
581 Thermophysical Properties. *J. Phys. Chem. A* **2012,** *116*, (44), 10810-10825.
582 57. Yang, F. X.; Ding, J. J.; Huang, W.; Xie, W.; Liu, W. P., Particle Size-Specific Distributions
583 and Preliminary Exposure Assessments of Organophosphate Flame Retardants in Office Air
584 Particulate Matter. *Environ. Sci. Technol.* **2014,** *48*, (1), 63-70.
585 58. Martonen, T. B.; Barnett, A. E.; Miller, F. J., Ambient Sulfate Aerosol Deposition in Man -
586 Modeling the Influence of Hygroscopicity. *Environ Health Persp* **1985,** *63*, (Nov), 11-24.
587 59. Hayes, D., Jr.; Collins, P. B.; Khosravi, M.; Lin, R. L.; Lee, L. Y., Bronchoconstriction
588 triggered by breathing hot humid air in patients with asthma: role of cholinergic reflex. *Am J Respir*
589 *Crit Care Med* **2012,** *185*, (11), 1190-6.
590 60. Donaldson, K.; Gilmour, M. I.; MacNee, W., Asthma and PM10. *Respir Res* **2000,** *1*, (1), 12-
591 5.
592 61. Halwani, R.; Al-Muhsen, S.; Hamid, Q., Airway remodeling in asthma. *Curr. Opin.*
593 *Pharmacol.* **2010,** *10*, (3), 236-45.
594 62. Hogg, J. C.; Timens, W., The pathology of chronic obstructive pulmonary disease. *Annu Rev*
595 *Pathol* **2009,** *4*, 435-59.
596 63. Matsumoto, H.; Niimi, A.; Tabuena, R. P.; Takemura, M.; Ueda, T.; Yamaguchi, M.;
597 Matsuoka, H.; Jinnai, M.; Chin, K. Z.; Mishima, M., Airway wall thickening in patients with cough
598 variant asthma and nonasthmatic chronic cough. *Chest* **2007,** *131*, (4), 1042-1049.
599 64. van den Berge, M.; ten Hacken, N. H.; van der Wiel, E.; Postma, D. S., Treatment of the
600 bronchial tree from beginning to end: targeting small airway inflammation in asthma. *Allergy* **2013,**
601 *68*, (1), 16-26.
602 65. Hogg, J. C.; Chu, F.; Utokaparch, S.; Woods, R.; Elliott, W. M.; Buzatu, L.; Cherniack, R.
603 M.; Rogers, R. M.; Sciurba, F. C.; Coxson, H. O.; Pare, P. D., The nature of small-airway obstruction
604 in chronic obstructive pulmonary disease. *New Engl J Med* **2004,** *350*, (26), 2645-2653.
605 66. Mason, J., Physics of Cloud and Precipitation. *B Am Meteorol Soc* **1971,** *52*, (12), 1209-&.